J Mater Sci (2006) 41:5870–5881
DOI 10.1007/s10853-006-0325-z

Influence of thermal treatment on the water release and the glassy structure of perlite

M. Roulia · K. Chassapis · J. A. Kapoutsis · E. I. Kamitsos · T. Savvidis

Received: 16 June 2004 / Accepted: 15 September 2005 / Published online: 29 June 2006

Abstract The effect of slow and rapid thermal treatment on water release and the structure of perlite was investigated by employing complementary techniques including X-ray diffraction, infrared spectroscopy and scanning electron microscopy. The study of several perlite samples, with different grain size and origin, has shown that rapid heating has a more pronounced effect on the glassy structure and that this is the only process capable of leading to perlite grain expansion. This process was simulated in a laboratory furnace allowing the careful control of temperature and time of treatment, and, thus, the description of their influence on the expansion process. The results show that molecular water released between 250 and 550 °C affects mostly the expansion process. Infrared spectroscopy provides evidence for additional water release, through dehydroxylation of Si–OH bonds, that may contribute also to expansion with a simultaneous development of the silicate network. The grain morphology was found to correlate with the expansion ratio. The presence of crystallites in raw perlite was shown to affect also the expansion process.

Dedicated to the memory of Professor D. Katakis

M. Roulia (✉) · K. Chassapis
Chemistry Department, Inorganic Chemistry Laboratory, University of Athens, Panepistimiopolis, Athens 157 71, Greece
e-mail: roulia@chem.uoa.gr

J. A. Kapoutsis · E. I. Kamitsos
Theoretical and Physical Chemistry Institute, National Hellenic Research Foundation, 48 Vass. Constantinou Ave., Athens 116 35, Greece

T. Savvidis
General State Chemistry Laboratory, Kozani Branch, Kozani 501 00, Greece

Introduction

Perlite is a glassy volcanic rock of rhyolitic composition containing 2–5 wt% water. When perlite is heated rapidly in the range 700–1,000 °C it expands 10–15 times its original volume and leads to a lightly colored frothy material, expanded perlite.

During the expansion process the grains start to soften superficially. At the pyroplastic stage, the water trapped into the inner layers of grains starts to evaporate and pushes its way out, resulting in the expansion of grains. Water plays the most important role in the expansion process not only by expanding the grain during evaporation but also by reducing the viscosity of the softened grain [1]. Expanded perlite exhibits increased porosity and decreased density. Representative values of density for crude, crashed and expanded perlite are 2.2–2.4, 0.9–1.1 and 0.6–1.2 kgm^{-3}, respectively.

Expanded perlite is versatile and floats, exhibits low thermal conductivity, high absorption of sound and resistance to fire. It is used mostly in the construction industry, in agriculture, as a filtering aid, as an adsorbent material and for environmental purposes e.g. for combating oil spills.

In industry, perlite is expanded in horizontal rotary or stationary furnaces or, mainly, in vertical expansion furnaces. Numerical simulations [2–4] as well as a theoretical analysis [5] of the expansion process have been reported for vertical furnaces. It was suggested that expansion occurs in less than 3 s after perlite is inserted into the high temperature furnace [2]. Although expansion is the most important treatment of perlite, research work on perlite is devoted mainly to properties [6–9] and potential uses [10–18] of this material. However, questions related to structural changes induced by thermal treatment, that may support a mechanism of expansion at a molecular level, remain open.

Water in perlite is present as molecular water and as hydroxyl groups [19]. Water in the form of hydroxyl groups bound to silicon atoms (i.e. in Si–OH bonds) is introduced into the silicate network under hydrothermal conditions [20]. The number of hydroxyl groups per silicon atom affects directly the connectivity of the perlite network, and this is usually expressed in terms of the Q_n silicate tetrahedral units with n being the number of oxygen atoms bridging two silicon centers (Fig. 1). The concentration of hydroxyl groups in perlite increases with total water content. For total water content over 3 wt% the hydroxyl content may level off, while the concentration of molecular water increases [21]. In another study [22], six types of water were suggested in terms of the temperature release profile: (a) 80–150 °C, (b) 180–250 °C, (c) 280–400 °C, (d) 400–550 °C, (e) 650–800 °C, (f) > 800 °C.

In the present work, the mechanism of perlite expansion was investigated through examination of the effect of slow and rapid thermal treatment on the perlitic structure. The expansion process under thermal treatment was simulated in a laboratory furnace, so that time and temperature could be controlled and their influence on the process could be described. Moreover, the expansion occurs slower and hence the various stages can be studied. The dependence of the expansion process on water content, morphology of grains and presence of crystallites has been examined as well and the results are reported in this work.

Experimental section

Materials

Samples of raw and expanded perlite were provided by Silver and Baryte Ores Mining S.A. and originate from Provatas, Trachilas and Tsigrado regions of the Milos Island, Greece. Three different grain sizes of raw perlite were employed for our laboratory studies; the coarse, medium and fine grains with diameters of 2.5–0.8 mm, 1.2–0.15 mm and 0.6–0.15 mm, respectively. The 2.5–0.8 mm and 0.6–0.15 mm fractions have quite different grain sizes and were chosen in order to probe the effect of size on the water retention. On the other hand, the 1.2–0.15 mm fraction can be considered as intermediate, and as such it was selected for comparison purposes. Fine grains of raw perlite from Italy, Hungary, China and Turkey were also provided for the present study by Silver and Baryte Ores Mining S.A. The grain sizes of expanded perlite were coarse, medium and fine with 5.0–1.0 mm, less than 4.0 mm and less than 2.5 mm in diameter, respectively. All samples were used as received.

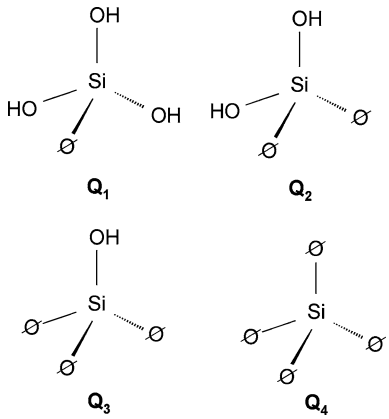

Fig. 1 Schematic structures of silicate tetrahedral units Q_n, with n denoting the number of oxygen atoms bridging two silicon centers (Ø = bridging oxygen atom)

Heat treatment

Measurements of the water content were performed in a laboratory furnace. Raw perlite samples were heat treated at 150, 250, 400, 550, 740 and 950 °C successively for 3.5 h at each temperature. The samples were weighed after each thermal treatment so that the amount of water evolved could be measured. The same procedure was repeated for 15 h of heat treatment at each temperature. Prior to all measurements the samples used for our experiments were kept dry under constant temperature.

In order to study the effect of slow thermal treatment on perlite, Trachilas' medium grains were heat treated with a heating rate of 10 °C/min, and samples were collected at 150, 250, 280, 500 and 740 °C (samples S1–S5, respectively). This thermal treatment was carried out in a programmable furnace using a Shimaden FP 21 Programmable controller.

The variation of the expansion ratio with time was studied by placing a Pt crucible loaded with Trachilas' medium grain perlite in a preheated laboratory furnace at 800, 900, 1,000, 1,100 and 1,200 °C. Heat treatment time in these experiments varied from 5 to 240 s. Similar expansion experiments were performed on raw perlite samples of different origin. The volumes of raw and expanded perlite were measured as apparent volumes using a volumetric cylinder and they were employed to determine the expansion ratio of perlite. This procedure, being quite different from the industrial process, requires higher temperatures but it offers the advantage of reproducible results and a good control of the parameters affecting expansion, e.g., time and temperature.

Characterization techniques

Thermal gravimetric and differential thermal analysis (TGA-DTA) measurements were performed on a Seiko 750 instrument, while a QuanX–Spectrace EDXRF instrument

was employed for elemental analysis of perlite samples. Scanning electron micrographs (SEM) were recorded on an environmental scanning electron microscope (XL/30 ESEM Philips). Prior to analysis the samples were coated with carbon to achieve sufficient electrical conductivity.

Infrared spectra were measured on a Fourier-transform vacuum spectrometer (Bruker 113v), which was equipped with special attachments allowing measurements in the diffuse reflectance and specular reflectance (11° off-normal) modes. Each spectrum represents the average of 200 scans recorded at room temperature with 2 cm^{-1} resolution.

For measurement of diffuse reflectance spectra, perlite was mixed with dry KBr (5 wt%) and the mixture was milled for 10 min in a vibrating mill to yield a fine homogeneous powder. This process ensures reproducible diffuse reflectance spectra, i.e. spectra free of particle size effects. The measured diffuse reflectance intensity was expressed in terms of the Kubelka–Munk function, $f(R)$, as follows:

$$f(R) = \frac{(1-R)^2}{2R}, \quad (1)$$

where R is the diffuse reflectance of the perlite/KBr mixture relative to the reflectance of dry pure KBr.

For specular reflectance measurements, perlite was milled without KBr and it was then pressed into a pellet. The specular reflectivity of the perlite pellet was measured relative to that of a high-reflectivity aluminum mirror. The reflectance data were analyzed by Kramers–Krönig transformation to obtain the frequency dependent phase angle between reflected and incident wave. The reflectivity and phase angle spectra were subsequently employed to calculate the optical and dielectric properties of samples [23]. Infrared data reported in the form of absorption coefficient spectra, $\alpha(v)$, were calculated from the relation:

$$\alpha(v) = 4\pi v\, k(v), \quad (2)$$

where $k(v)$ is the frequency-dependent imaginary part of the complex refractive index and v is the frequency in cm^{-1}.

Results and discussion

Chemical analysis and X-ray diffraction patterns

Raw perlite samples of different origin were analyzed and results are given in Table 1 in terms of oxides of the main elements present. Table 1 shows also a typical perlite composition expressed in mol percentage of each oxide. This chemical analysis suggests that perlite can be regarded as a negatively charged aluminosilicate network balanced by various metal cations.

Information on the amorphous/crystalline nature of the perlitic network can be extracted from X-ray diffraction (XRD) patterns. It is noted that the expansion process leads to a part of perlite remaining unexpanded. After separation by floatation the lighter expanded perlite can be removed and the residual unexpanded perlite can be filtered out. Figure 2 shows results of XRD measurements on raw perlite (Trachilas' medium grains), as well as on the expanded and unexpanded fractions of the thermally treated material. Figure 2a suggests that the raw material is mostly amorphous in nature, with small amounts of feldspar (F), quartz (Q) and biotite (B) crystallites. The presence of crystallites in raw perlite is correlated to the origin of perlite, with more crystallites being formed in the case of slow freezing of lava. While the expanded fraction of perlite (Fig. 2b) is clearly amorphous, the unexpanded perlite (Fig. 2c) comprises the crystallites present in the raw material and part of the amorphous phase. The chemical composition of expanded perlite samples, in terms of oxides of the main elements present, is presented in Table 1. Also, the unexpanded fraction contains slightly more Fe, Al, Ca and Si compared to the expanded perlite probably due to the presence of biotite,

Table 1 Chemical composition of raw perlite of different origin and an indicative mole percentage of the various oxides

Composition	Raw perlite (% w/w)									Expanded perlite (% w/w)		
	Trachilas	Provatas	Tsigrado	Italy	China	Hungary	Turkey	typical	% mol	coarse	medium	fine
SiO_2	74.2	73.4	73.2	69.7	71.4	73.5	71.0	71–76	72.9	74.2	74.5	74.9
Al_2O_3	12.02	12.36	11.92	14.06	12.37	12.07	12.77	12–16	8.1	13.05	12.68	12.88
K_2O	4.30	2.76	2.61	4.65	4.39	3.69	4.44	4–5	2.7	3.01	3.56	3.05
Na_2O	3.20	4.20	4.16	3.27	3.95	3.56	3.18	3–5	4.5	3.14	3.25	3.20
Fe_2O_3	1.45	1.81	1.81	2.08	1.13	1.85	1.64	0.8–1.5	0.3	1.50	1.24	1.64
CaO	0.85	1.32	1.34	0.82	1.03	1.34	0.93	0.5–1.4	0.9	0.96	0.77	1.00
MgO	0.25	0.28	0.30	0.35	0.25	0.27	0.40	0.2–0.5	0.5	0.27	0.21	0.26
H_2O	3.11[a]	2.18[a]	2.58[a]	3.75[a]	5.00[a]	3.50[a]	4.75[a]	3.0	10.1	1.62	1.88	1.72

Chemical composition of expanded perlite is included for comparison

[a]Fine grains

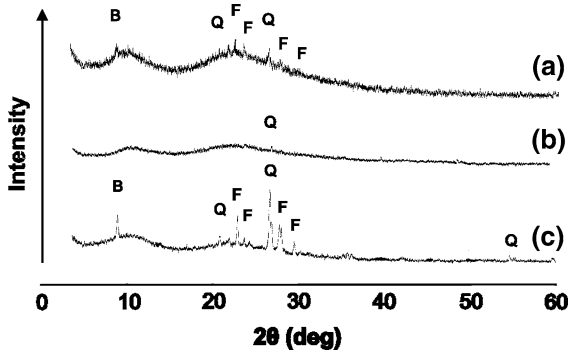

Fig. 2 XRD diagrams of Trahilas' medium grain perlite in the raw (**a**), expanded (**b**) and unexpanded (**c**) states, with B, F and Q denoting the presence of biotite, feldspar and quartz, respectively

feldspar and quartz. Therefore, both XRD and chemical composition results suggest that expansion takes place only in the amorphous phase of raw perlite. It was observed also that two or more particles are often produced during the expansion of a single grain. Apparently, small crystallites located inside the amorphous domain cause splitting by preventing the expansion of the grain as a whole.

Water release by thermal treatment of perlite

The amount of water released from perlite by thermal treatment for 3.5 and 15 h at various temperatures is presented in Table 2 for different samples of raw and expanded perlite. It is reasonable to assume that the relatively loosely bound water is released at lower temperatures. In Table 2, the amount of water released is expressed as percentage of total water. For each perlite sample, the amount of water released by 3.5 h thermal treatment at 950 °C was found equal to that released by extended treatment (15 h) at the same temperature, and, thus, this water content is described as ''total water'' of perlite (second column in Table 2). It is important to notice that expanded perlite still retains some water (1.6–1.9 wt%), although less than that in raw perlite (2.0–5.0 wt%) for all temperatures studied in this work. The total water content tends to decrease with decreasing grain size for raw perlite; the opposite trend being observed for expanded perlite. For the raw fine-gain perlite samples studied here the water content varies with origin of perlite in the order: Chinese > Turkish > Italian > Hungarian > Greek.

Consequently, the differences observed in Table 2 depend on the origin of the sample, the grain size, the temperature and the heating time. Especially for samples of the same origin, it is clear from the results in Table 2 that the grain size plays a crucial role in the water release at all temperatures and times selected. In general, the fine grains of raw perlite contain smaller quantities of physically retained water, simply due to the grinding procedure. Thus, reduced amounts of released water is expected for fine grains of raw perlite at low temperatures. In contrast, the remaining water is more strongly bound and, as the temperature is raised, the effect of the grain size becomes negligible. The opposite stands for expanded perlite; the effect of the expansion is more pronounced in the case of fine grains compared to the case of coarse grains. Therefore, the water retained in fine grains can be released more readily at low temperatures.

Table 2 Water release (± 5%) by heat treatment at different temperatures of raw and expanded perlite

Perlite sample	Total water (w/w)	Water release (%)											
		150 °C		250 °C		400 °C		550 °C		740 °C		950 °C	
		3.5 h	15 h	3.5 h	15 h	3.5 h	15 h	3.5 h	15 h	3.5 h	15 h	3.5 h	15 h
Raw													
Trachilas (C)	3.25	7.7	11.4	44.9	56.0	76.3	80.0	89.8	89.8	99.7	99.7	100	100
Trachilas (M)	3.48	6.9	13.8	45.4	56.0	75.6	77.6	88.8	88.8	92.8	92.8	100	100
Trachilas (F)	3.11	0.47	0.89	35.0	50.5	80.1	84.2	87.1	87.1	100	100	100	100
Provatas (C)	2.60	0.65	4.6	33.5	57.7	74.6	86.5	93.8	93.8	100	100	100	100
Provatas (M)	2.24	0.62	0.90	21.9	38.0	66.1	77.2	77.2	82.6	88.8	100	100	100
Provatas (F)	2.18	0.57	0.85	17.0	28.4	62.8	68.8	78.4	83.9	91.3	91.3	100	100
Tsigrado (C)	3.17	6.6	7.9	31.6	63.2	71.1	78.9	78.9	82.9	94.7	94.7	100	100
Tsigrado (M)	2.92	7.1	12.9	30.0	57.2	60.0	70.0	85.7	87.1	94.3	94.3	100	100
Tsigrado (F)	2.58	6.5	12.9	29.4	48.4	66.1	71.0	87.1	87.1	98.4	98.4	100	100
Italy (F)	3.75	8.8	15.6	20.0	62.1	66.7	82.2	85.6	92.2	93.3	94.4	100	100
Hungary (F)	3.50	1.1	7.1	19.1	59.5	64.3	80.9	85.7	92.9	95.2	95.2	100	100
China (F)	5.00	10.0	11.7	41.7	68.3	75.0	81.7	89.2	94.2	96.7	96.7	100	100
Turkey (F)	4.75	7.0	12.3	35.1	68.4	72.8	79.8	89.5	94.7	96.5	96.5	100	100
Expanded													
Expanded (F)	1.88	46.3	46.3	72.4	74.0	79.8	79.9	81.5	81.5	82.6	82.6	100	100
Expanded (M)	1.72	35.1	38.8	59.6	59.6	74.5	75.6	78.8	78.8	80.9	80.9	100	100
Expanded (C)	1.62	26.1	30.2	51.0	51.6	58.4	71.3	77.5	77.5	79.6	79.6	100	100

Amount of water released is expressed as percentage of total water (w/w). Note: C = coarse, M = medium, F = fine

In the case of raw perlite, the water released during 3.5 h of treatment at temperatures in the ranges 0–250 °C (type A), 250–550 °C (type B), and 550–950 °C (type C) represents ca. 20–45%, 45–65% and 5–20% of the total water content, respectively (Fig. 3a). In the case of 15 h of thermal treatment the water amount of types A and B is reversed (ca. 40–70% and 20–50% of the total, respectively) while type C remains almost constant (Fig. 3b).

The classification of water in the above categories on the basis of the release temperature reflects the types of water bound in the perlitic network. Therefore, water of type A represents the molecular water bound loosely either superficially or adsorbed in pores. Type B accounts for water volatile at 250–550 °C, and this is present as –OH groups and as molecular water trapped into the inner pores of the material. Type C describes –OH groups associated to oxygen atoms through strong hydrogen bonding, e.g. –OH groups bound to nonbridging oxygens [22]. Each temperature band includes a number of experimentally observed water release processes with similar distinct characteristics.

In all cases of raw perlite, 80–95% of total water has been released below 550 °C. The above discrimination of

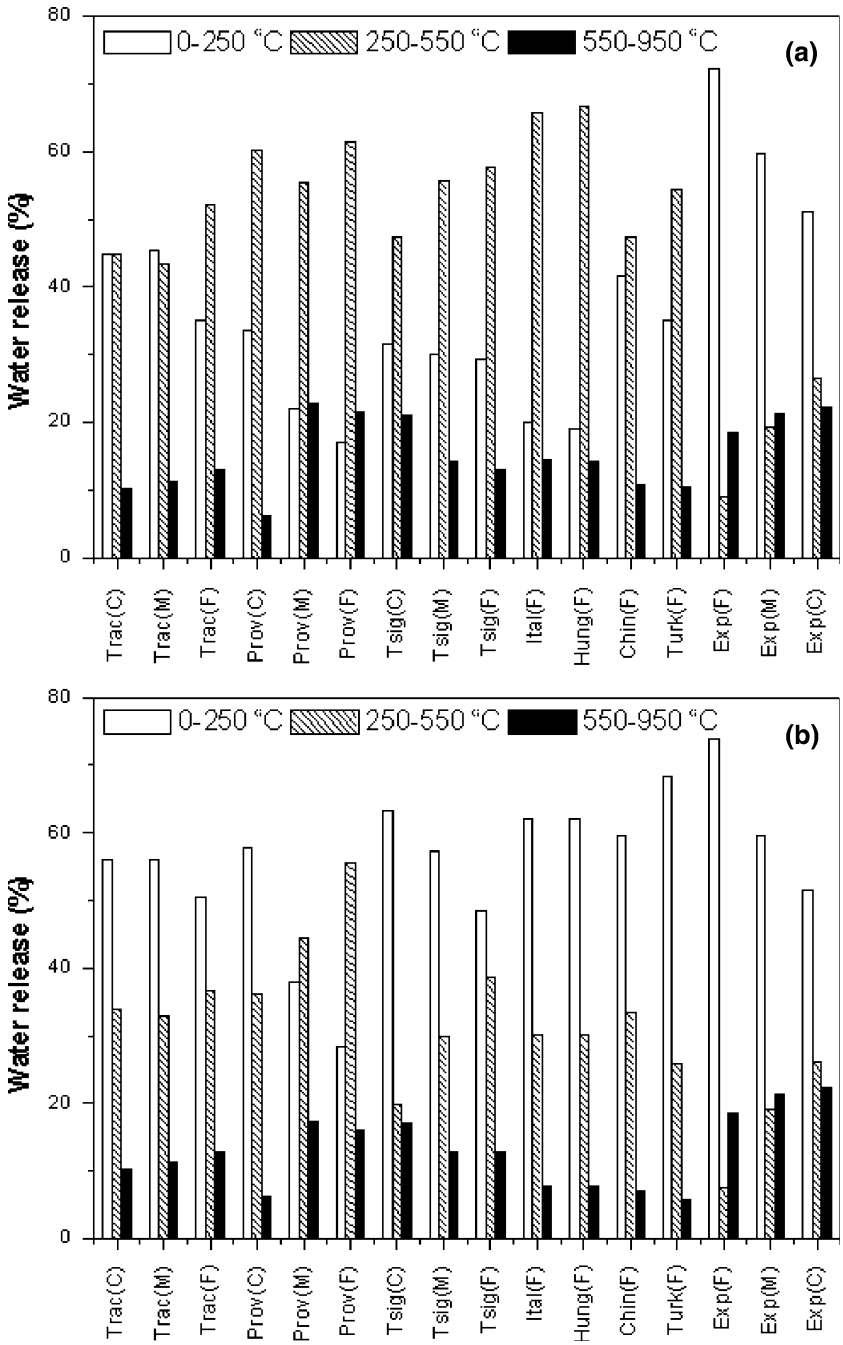

Fig. 3 Water release (% of total water) for raw and expanded perlite in the temperature ranges 0–250 °C, 250–550 °C and 550–950 °C. Heat treatment was conducted at temperatures specified in Table 2 for 3.5 h (**a**) and for 15 h (**b**). For the notation of the origin of raw and expanded perlite samples see also Table 2

the total water into types A, B and C is useful because it shows that a 20–30% of the total water may evolve at a different temperature range upon thermal treatment of perlite, and this amount depends on time and temperature of heat treatment, i.e. the higher the temperature the shorter the time.

In the case of expanded perlite (Fig. 3a, b) there is a significant change in percentages of types A, B and C of the water content. Specifically, type A is significantly increased (ca. 50–70% of total), type B is decreased (ca. 10–25%) and type C remains practically unchanged (about 20%), the results being almost the same for 3.5 and 15 h of heat treatment. It can be suggested that molecular water trapped into the inner pores of raw perlite manages to escape during the expansion process, while the rest remains in expanded perlite. Since expanded perlite has a significantly more open structure compared to the raw material, most of the remaining water becomes now accessible for release under thermal treatment at lower temperatures. Therefore, certain types of water initially present in raw perlite (e.g., of type B) may function as water of apparent type A in the expanded perlite. This may also explain the fact that expanded perlite still retains some loosely bound water.

The TGA-DTA curves in Fig. 4 are typical of all raw and expanded perlite samples examined. The results from thermogravimetric analysis are fully consistent with those obtained from heating the samples in a laboratory furnace; the water release from 250 to 550 °C in expanded perlite is significantly less than that in raw perlite. At this temperature range, the reduction of water released from expanded perlite is attributed to water losses occurred during the expansion process. This is in accordance with the results of Lehman and Rössler [22] who found that the removal of the water evolved between 250 and 550 °C impairs the expansion of perlite. Moreover, Lehman and Rössler have observed that norite and obsidian, where the water becomes volatile above 600 °C, showed no expansion.

It is obvious from Fig. 4 that the temperature range limits cannot be strictly set due to both the complexity of the material and the variety of interactions between water/–OH groups and the matrix.

Infrared spectra of slow and rapidly heat-treated perlite

The effect of thermal treatment on perlite was monitored also by infrared spectroscopy. For this purpose, raw perlite from Trachilas (Milos, Greece) was heat treated at a rate of 10 °C/min in a programmable furnace and samples of material were collected at temperatures 150 °C (S1), 250 °C (S2), 280 °C (S3), 500 °C (S4) and 750 °C (S5). The heating rate employed in this study is much slower

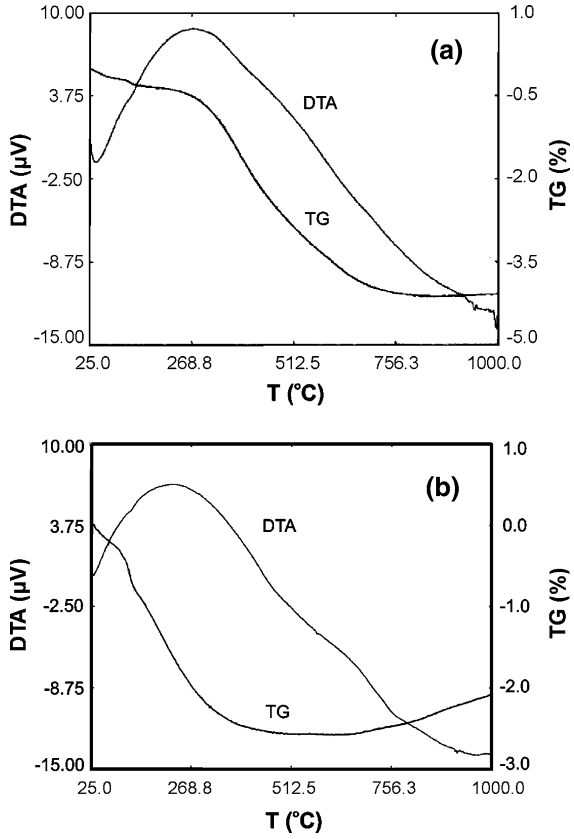

Fig. 4 Typical TGA-DTA curves for raw (**a**) and for expanded (**b**) perlite. Trachilas raw perlite (medium grains) and expanded medium grains were used

compared to that during the expansion process, and, thus, it does not cause expansion of perlite.

Figure 5 depicts the diffuse reflectance spectra of samples S1–S5 in two spectral ranges of interest to water release under thermal treatment. It is noted that the spectrum of raw perlite, being almost identical to that of sample S1, was not included in Fig. 5 for reasons of clarity. The deformation mode of molecular water gives a well defined peak at ca. 1,630 cm^{-1} (Fig. 5a), while the broad and asymmetric absorption envelope ranging from ca. 2,800 to 3,800 cm^{-1} (Fig. 5b) arises from O–H stretching vibrations in a variety of environments [24, 25]. In particular, the O–H stretching of free silanol groups (Si–OH) is responsible for the relatively sharper feature at higher frequencies (ca. 3,605 cm^{-1}), while hydrogen-bonding results in the weakening of the O–H bond and the shift of its stretching frequency to lower values. Thus, hydrogen-bonded O–H groups should be responsible for shoulders at ca. 3,430 and 3,270 cm^{-1} in Fig. 5b. Such hydrogen-bonding could be between neighboring silanols or molecules of adsorbed water, or between neighboring silanol and adsorbed water molecules. As seen in Fig. 5, the change of the O–H related absorption profiles in samples S1 to S3 is relatively small in both frequency ranges, but it becomes pronounced for

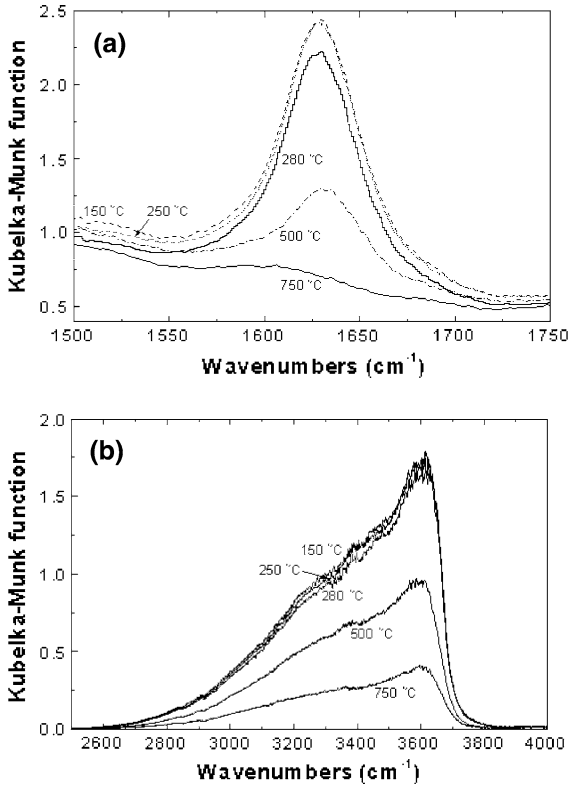

Fig. 5 Effect of thermal treatment on raw perlite (Trachilas medium grains) probed by FT-IR diffuse reflectance spectroscopy. Infrared intensity is expressed as Kubelka–Munk function. The spectral regions of molecular water deformation and stretching vibration of O–H groups are shown in (**a**) and (**b**), respectively

samples S4 and S5. In addition, while the 1,630 cm^{-1} band of molecular water has almost vanished in the spectrum of sample S5 (Fig. 5a, 750 °C), the O–H stretching envelope of the same sample retains considerable intensity (Fig. 5b, 750 °C). This finding indicates that, under the thermal treatment of perlite employed here, molecular water is being released faster compared to that present in the form of hydroxyl groups in Si–OH bonds.

In order to investigate the effect of water release on the silicate backbone of samples S1–S5 their specular reflectivity spectra were measured and are presented in Fig. 6, in a range where the main vibrational modes of the silicate network are active. Even though the overall reflectivity profiles do not reveal any obvious change upon water release, the value of absolute reflectivity decreases from sample S1 to S4 (500 °C) and then increases again for S5 (750 °C). This effect may be attributed to changes in sample porosity that accompany the release of water. In particular, heat treatment in the range 150 to 500 °C appears to result into a more open porous structure that scatters effectively the infrared light, while treatment at 750 °C leads to a relatively more compact silicate network structure [26].

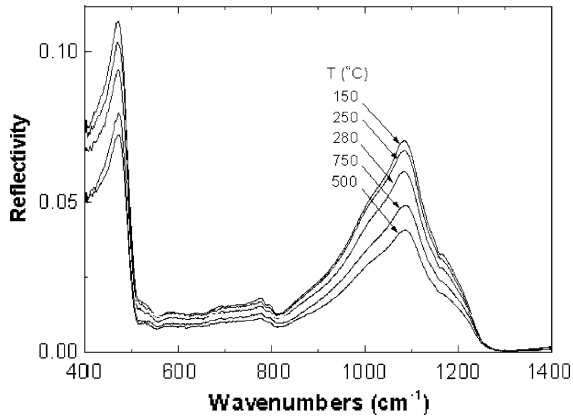

Fig. 6 FT-IR specular reflectance spectra of raw perlite thermally treated at various temperatures

Structural changes at the molecular level can be tracked better through absorption spectra because they depend only on the imaginary part of the complex refractive index (Eq. (2)), as opposed to reflectivity spectra which depend in a complex manner on both real, $n(\nu)$, and imaginary part, $k(\nu)$, of the refractive index [23]. The calculated absorption coefficient spectra of perlite samples S1–S5 are shown in Fig. 7, where they have been scaled on their strongest envelope from 900 to 1,300 cm^{-1} to facilitate comparison. Besides this absorption feature, all spectra exhibit additional bands peaking at ca. 470 and 785 cm^{-1}. Bands at similar frequencies in the case of vitreous silica and modified silicate glasses have been assigned to characteristic vibrations of the silicate network [26, 27]. In particular, the band at ca. 470 cm^{-1} was attributed to the rocking motion of the bridging oxygen atom perpendicular to the Si–O–Si plane; the weak band at 785 cm^{-1} was assigned to the bending motion of the oxygen atom along the bisector of the Si–O–Si bridge, while the intense band at

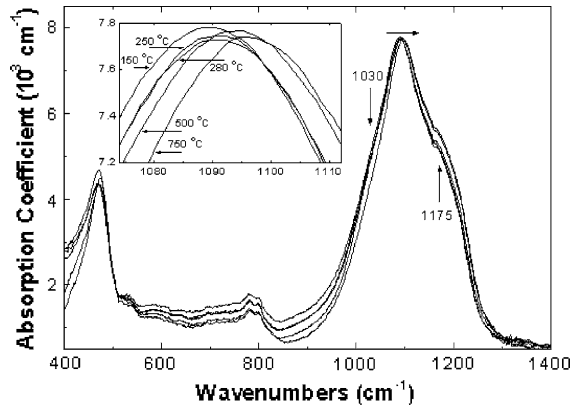

Fig. 7 Absorption coefficient spectra of raw perlite thermally treated at various temperatures. Note that spectra were normalized with respect to the band at ca. 1,090 cm^{-1} to allow comparison. The inset shows expanded the maximum absorption at ca. 1,090 cm^{-1} to highlight the effect of thermal treatment

ca. 1,090 cm^{-1} (accompanied by a shoulder at *ca.* 1,175 cm^{-1}) has been attributed to asymmetric stretching vibrations of Si–O–Si bridges. Such Si–O–Si bridges can be broken either by creation of non-bridging oxygen atoms in $Si–O^-$ bonds which are charge compensated by metal ions, or by hydrolysis effects leading to formation of Si–OH bonds in Q_n structures (Fig. 1). Both effects cause the progressive ''depolymerization'' and, thus, weakening of the silicate network and this is manifested by the broadening of the 900 to 1,300 cm^{-1} infrared envelope and shifting of its absorption maximum towards lower frequencies. In this respect, the shoulder at ca. 1,030 cm^{-1} may signify the presence of Q_2 species, while the main band at ca. 1,090 cm^{-1} is characteristic of Q_3 tetraherdal units in perlite. The presence of a considerable amount of aluminum in the composition of perlite (about 8 mol% Al_2O_3, Table 1) suggests the formation of mixed Si–O–Al bridging bonds as well. It should be noted that bonding of aluminum to silicon in the form of Si–O–Al bonds is expected to affect the 900–1,300 cm^{-1} envelope in the same manner as the Q_n silicate tetrahedral units having Si–OH bonds or non-bridging oxygen atoms [28]. However, since thermal treatment of perlite does not affect its aluminum to silicon ratio, thermally-induced changes of the absorption spectra can be attributed mainly to variations in the relative population of the Q_n silicate species.

On this basis, we discuss now the effect of heat treatment on the perlitic microstructure. As seen in Fig. 7, increasing temperature of treatment affects the 900 to 1,300 cm^{-1} envelope in a very systematic way. Thus, the relative intensity of the ca. 1,030 cm^{-1} shoulder decreases, and this is followed by a parallel increase of the relative intensity of the shoulder at ca. 1,175 cm^{-1} and a frequency upshift of the absorption maximum at ca. 1,090 cm^{-1}. This frequency upshift is seen better in the inset of Fig. 7, and corresponds to ca. 7 cm^{-1} from sample S1 (150 °C) to S5 (750 °C). Such temperature-induced spectral variations can be understood in terms of a decrease of the relative abundance of Q_2 structural units in favor of Q_3 and Q_4 structures, i.e. towards a more cross-linked, or more ''polymerized'', silicate network structure. These structural changes become more pronounced for samples S4 and S5 that were treated at the relatively elevated temperatures of 500 and 750 °C, respectively. Thus, even at low heating rates of raw perlite that cause no expansion, the release of water induces changes in both porosity of material and connectivity of its silicate structure.

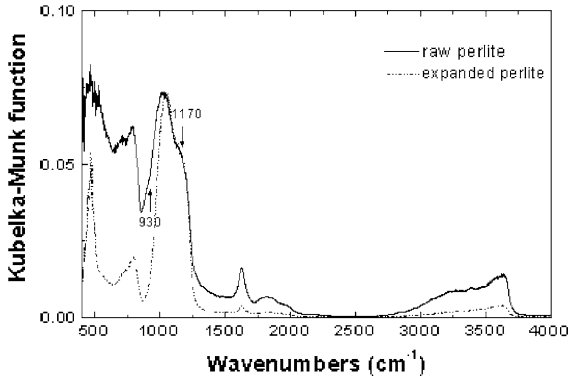

Fig. 8 FT-IR diffuse reflectance spectra of raw and expanded perlite

The extent of structural changes occurring as a result of perlite expansion were probed by FT-IR diffuse reflectance spectroscopy, and typical results are shown in Fig. 8 for raw and expanded perlite from the Trachilas region. Spectral comparison shows that expanded perlite retains some water as indicated by the non vanishing infrared intensity at 1,630 cm^{-1} and the weak absorption profile in the range 2,800 to 3,800 cm^{-1}. The shoulder at ca. 930 cm^{-1} in the spectrum of raw perlite is typical of the Si–O stretching vibration in Si–OH bonds [26]. This feature is also suppressed in the spectrum of expanded perlite, suggesting the condensation of Si–OH bonds into Si–O–Si linkages upon water elimination, and, thus, the development of a better cross-linked silicate network. Increasing cross-linking of the silicate structure is consistent also with the shift of the 900–1,300 cm^{-1} envelope of raw perlite by about 20 cm^{-1} after expansion. This frequency shift is greater than that observed in the slow thermally-treated samples S1–S5 (shift by ca. 7 cm^{-1}), suggesting a larger extent of structural changes upon perlite expansion.

Based on the above spectral observations for both slow and rapidly heat treated perlite, we propose that the release of adsorbed molecular water is followed at increasing temperatures by additional water elimination through condensation of Si–OH bonds into Si–O–Si linkages. A possible scheme describing this process is given below:

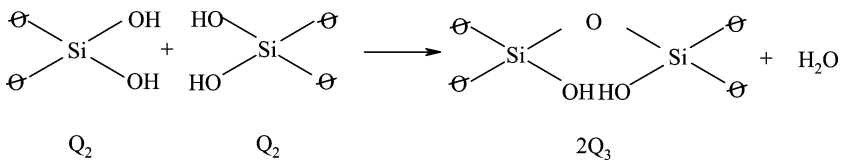

It is noted that complete elimination of –OH groups from Q_n silicate species would lead to their condensation into a three dimensional silicate structure based on inter-

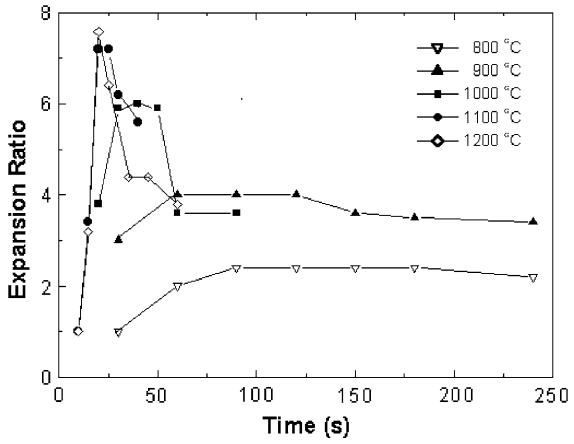

Fig. 9 Effect of thermal treatment time on the expansion ratio of perlite treated in a laboratory furnace preheated at the specified temperatures

linked Q_4 tetrahedral species. Such a complete water release reaction could be $2Q_2 \rightarrow 2Q_4 + 2H_2O$.

Conditions for optimum perlite expansion

Raw perlite samples (Trachilas' medium grains) were expanded in a laboratory furnace at temperatures 800, 900, 1,000, 1,100 and 1,200 °C. Figure 9 shows the effect of heat treatment time on the expansion ratio, V_{exp}/V_{raw}, with V_{raw} and V_{exp} denoting the volume of sample before and after expansion, respectively. There seems to be an optimum time range for achieving the maximum expansion ratio at each temperature, e.g. at 1,000 °C the highest expansion ratio is reached within a 20 s critical period between ca. 30 and 50 s.

As temperature increases, this critical time range decreases significantly and shifts towards lower heating times. Thus, for 1,200 °C the critical heat treatment time is less than 5 s and this is centered on 20 s. Outside the critical time limits the expansion ratio decreases. A possible explanation is that during the early stages of thermal treatment the temperature inside the grains is relatively low and the viscosity is still high. Furthermore, only a small part of water has been yet removed resulting in low expansion ratios. At all temperatures, perlite starts to shrink beyond the critical time range due to both its softening and superficial fusion.

The optimum time ranges were employed to achieve the maximum expansion ratio at each temperature for various raw perlite samples, and typical results are shown in Table 3. The data suggest that for samples of the same origin the expansion ratio tends to increase in most cases upon increasing the size of perlite grains. For the fine grain samples the expansion ratio was found to vary with the origin of perlite as follows: Italian < Chinese < Hungarian < Greek < Turkish; this trend being retained for all temperatures considered in this study.

Figure 10 presents the maximum expansion ratio values as a function of total water content for fine grain perlite samples. The three samples from Greek sites and the one from the Turkish site (points a to d in Fig. 10) support a monotonic increase of expansion ratio with total water content. The rest of perlite samples, i.e. of Hungarian, Italian and Chinese origin, seem to drop of this apparent correlation. To find possible causes of such differences, we compare in Fig. 11 the infrared absorption spectra of the later three samples and of two samples correlated in Fig. 10 (samples from Tsigrado and Turkey). The spectra have been scaled on the their high intensity band at ca. 1,100 cm^{-1} to allow comparison, and are shown in the expanded 800 to 1,300 cm^{-1} region that reflects microstructural characteristics of the silicate network.

Table 3 Expansion ratio (± 4%) of various perlitic samples at different temperatures

Sample	Grain size	Expansion Ratio				
		800 °C	900 °C	1,000 °C	1,100 °C	1,200 °C
Trachilas	Coarse	2.60	4.03	7.00	8.60	9.73
	Medium	2.40	3.93	6.00	7.20	7.87
	Fine	2.50	4.63	6.30	8.40	8.87
Provatas	Coarse	2.10	4.65	6.60	8.97	8.93
	Medium	2.10	4.51	6.33	7.60	7.33
	Fine	1.90	4.32	5.50	6.33	7.27
Tsigrado	Coarse	2.40	4.60	6.67	8.33	7.47
	Medium	2.30	4.15	6.03	7.13	7.40
	Fine	2.33	4.40	5.90	6.50	7.20
Italy	Fine	1.60	2.47	3.47	3.70	4.40
China	Fine	2.04	2.98	3.81	4.23	4.60
Hungary	Fine	3.10	4.28	5.83	6.80	6.40
Turkey	Fine	3.00	5.12	9.74	12.17	10.67

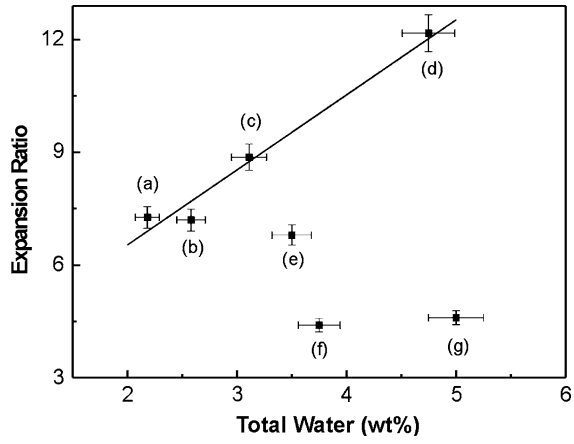

Fig. 10 Effect of total water content on the maximum expansion ratio for fine gain perlite samples of different origin (a: Provatas, b: Tsigrado, c: Trachilas, d: Turkey, e: Hungary, f: Italy and g: China). The solid line represents least squares fitting for data points (a) to (d)

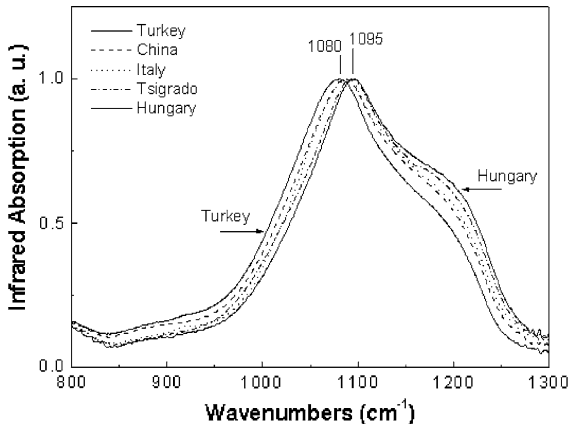

Fig. 11 Comparison of infrared absorption spectra in the 800–1,300 cm^{-1} range for fine-grained raw perlite samples of different origin (see legend). The spectra were normalized with respect to the band at ca. 1,090 cm^{-1} to highlight differences originating from silicate microstructural variations

It is observed that for the sample of Turkish origin the absorption maximum appears at relatively low frequency (ca. 1,080 cm^{-1}), and its shoulder at ca. 1,175 cm^{-1} shows the smaller relative intensity compared to the rest of samples. Based on the discussion of the previous section, it is suggested that the sample of Turkish origin manifests characteristics of a relatively more ''depolymerized'' or less cross-linked silicate network compared to the rest of samples. The samples from Tsigrado and Hungary reveal a relatively less ''depolymerized'' silicate network, while the Chinese and Italian samples fall in between the samples from Turkey and Tsigrado.

It is noted that these trends in silicate microstructural characteristics are generally consistent with differences in water content of the samples considered here. Therefore, we conclude that water content and silicate microstructure, while both being important for the perlite expansion process, cannot account fully for the maximum expansion ratio values depicted in Fig. 10. For this reason, perlite characteristics were considered at a higher structural level and results are presented in the following section in terms of perlite grain morphology.

Grain morphology

Scanning electron microscopy (SEM) was employed to study the grain morphology of raw perlite samples and changes induced by expansion. Figure 12a–e display stages of the expansion process in the case of Trachilas' fine grains. The raw material is pumiceous with large vesicles (Fig. 12a). At the first stage of heat treatment (Fig. 12b) the grain starts to soften superficially and the outershell becomes smooth, while water trapped into the inner layers tries to escape and slightly blows up the grain as shown by the cracks developed on the surface. At a later stage, the grain is significantly blown up causing an opening of the structure and bubbles start to appear on the surface (Fig. 12c) serving as escape routes for water. Immediately afterwards, many bubbles have formed and also small holes are present (Fig. 12d). The small holes are sites of escape of the water. Finally, expansion of perlite occurs, where the grains explode violently and the morphology changes considerably as shown in Fig. 12e. In some cases the water escape routes may remain intact after expansion and hence whole bubbles appear in expanded perlite. The stages considered above for perlite of Trachilas' origin were found to be independent of the origin and the expansion ratio of the samples. Figures 12a–e prove that the expansion process starts from the inner layers of grains.

As was earlier noted, overheating of perlite, i.e. beyond its optimum time range leading to maximum expansion, results in the shrinking of grains. In the lower part of Fig. 12f the texture changes caused by the overheating are depicted and actually verify that the superficial melting is responsible for the expansion ratio decrease.

Considering the morphology of perlite, all Greek samples were found to be vesicular/pumiceous as shown by the typical example in Fig. 12a. Perlitic samples showing the lowest expansion ratio (i.e. Italian, Chinese and Hungarian) were characterized as mostly granular (Fig. 12g), while the Turkish perlite exhibiting the maximum expansion ratio shows an onionskin type morphology (Fig. 12h). Therefore, it is suggested that an important factor affecting the ability of grains to expand is the grain morphology, which manifests differences in the conditions of perlite formation, e.g. temperature and viscosity of lava and its quenching rate, and may reflect the easiness or difficulty in the formation of escape routes for the water gas released during rapid thermal treatment. Water released from granular grains, having small and well dispersed voids, such as those of Fig.12g, can escape easily, and, thus, this requires a small degree of perlite expansion. On the other hand, the water vapor developed in onionskin-like perlite cannot easily escape through the successive onionskin-like layers and, therefore, the sudden evaporation results in increasing pressure that blows up the grain until it finally explodes (expansion of the grain). This is a process with a relatively larger degree of difficulty, and, thus, its facilitation would require a larger expansion of the perlite structure. With regards to this point, it is noted that 5 s after the insertion of perlite in the laboratory furnace at 1,100 °C most of Hungarian perlite was almost intact, while Greek perlite had reached the stage of Fig. 12b and the Turkish perlite the stage of Fig. 12c. In addition, under these laboratory expansion conditions, Turkish samples were observed to expand violently compared to the other samples, bursting out of the crucible.

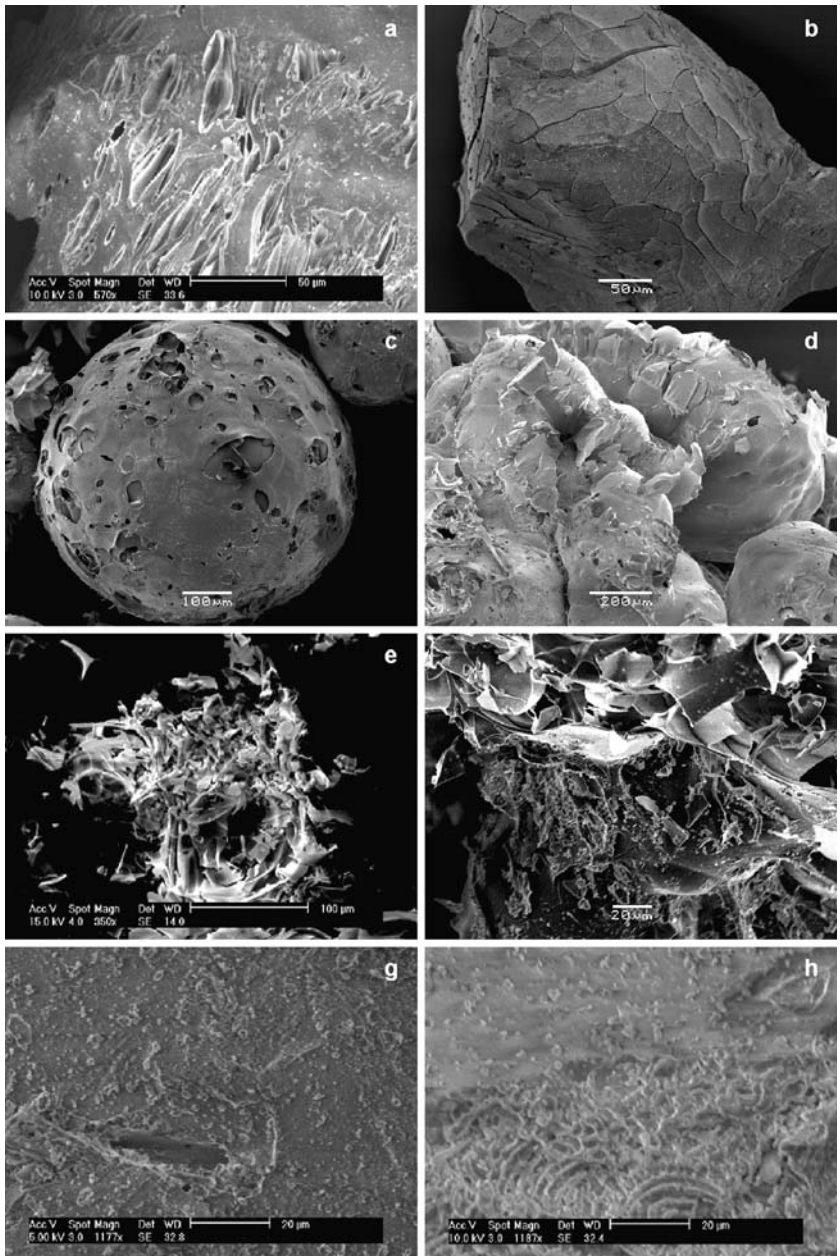

Fig. 12 Scanning electron micrographs of raw and expanded perlite: Greek raw pumiceous perlite (**a**), followed by various stages of expansion (**b**–**e**) and overheating (**f**); Hungarian raw perlite (**g**), and Turkish raw perlite (**h**)

Conclusions

It was shown in this work that raw perlite is dominated by an amorphous phase with inclusions of crystallites, which are formed during the slow freezing of lava. While the expansion of perlite, effected by rapid thermal treatment, is closely related to its amorphous phase, crystallites do not expand and are rejected as unexpanded perlite.

Both the expansion process and the slow thermal treatment (10 °C/min) result in the condensation of the glassy structure of perlite. Although the resulting effects are similar, silicate condensation occurring during expansion is more intense. The development of the silicate network has been attributed to dehydroxylation of mainly Si–OH groups and occurs during any thermal treatment (including thermal treatments that do not lead to expansion). This is the opposite reaction to the hydration procedure occurring to silicate glass under hydrothermal conditions [20] and has been correlated to the formation of perlite from natural rhyolitic glasses [29].

During the expansion process, starting from the inner layers of perlite, molecular water is released prior to any changes of silicate microstructure. As the temperature increases and grains start to soften, mostly type B of water (250–550 °C) starts to evaporate and pushes its way out. At first, water blows up the grain creating escape routes and

finally it explodes/expands the grain. In addition, terminal Si–OH groups are dexydroxylated with simultaneous water removal. This is identified in this work as a new category of water that may also contribute to the expansion of grains together with the rest of the ''effective water''. After expansion, perlite has an open structure and, thus, its remaining water becomes more readily accessible for release at lower temperatures.

It was also shown that there exists an optimum time range of heat treatment for obtaining the maximum expansion ratio at each temperature, while overheating was found to result in the shrinkage of grains. The expansion ratio determined at various temperatures was found to depend on grain size and origin of perlite. Besides the importance of total water content and silicate microstructure, the expansion ratio was found to depend on grain morphology of raw perlite. The granular type of morphology that has well dispersed microvoids allows water to escape easily, and, therefore, the corresponding expansion ratio is considerably smaller compared to that of perlite with vesicular/pumiceous and onionskin type morphology.

Acknowledgements This work was supported in part by the Greek General Secretariat for Research and Technology. Dr Y.D. Yiannopoulos is gratefully acknowledged for his help with infrared studies at NHRF.

References

1. Friedman I, Long W, Smith R (1963) J Geophys Res 68:6523
2. Zahringer K, Martin J-P, Petit J-P (2001) J Mater Sci 36:2691
3. Klipfel A, Founti M, Zahringer K, Martin J-P, Petit J-P (1998) Flow Turbul Combust 60:283
4. Zahringer K, Martin J-P, Petit J-P (2001) Glass Sci Technol 74:57
5. Papanastassiou D (1980) J Trans Inst Min Metall (Sect C: Mineral Process Extr Metall) 89:120
6. Dogan M, Alkan M, Chakir U (1997) J Colloid Interf Sci 192:114
7. Alkan M, Dogan M (1998) J Colloid Interf Sci 207:90
8. Laskowski JS (1993) J Colloid Interf Sci 159:349
9. Davis B, Mcphie J (1996) J Volcanol Geotherm Res 71:1
10. Tarasevich YI, Verlinskaya RM, Nesterova MP, Gornitskii AB (1986) Khimiya I Tekhnologiya Vody 8:34
11. Tarasevich YI, Panasevich AA, Bezorudko OV, Skrylev LD, Purich AA (1985) Khimiya I Tekhnologiya Vody 7:67
12. Roulia M, Chassapis K, Fotinopoulos C, Savvidis T, Katakis D (2003) Spill Sci Technol 8:425
13. Koumanova B, Peeva-Antova P (2002) J Hazard Mater A 90:229
14. Dogan M, Alkan M, Onganer Y (2000) Water Air Soil Poll 120:229
15. Khodabandeh S, Davis M (1997) Microporous Mater 9:161
16. Christidis GE, Paspaliaris I, Kontopoulos A (1999) Appl Clay Sci 15:305
17. Dogan M, Alkan M (2003) Chemosphere 50:517
18. Alkan M, Dogan M (2001) J Colloid Interf Sci 243:280
19. Sodeyama K, Sakka Y, Kamino Y (1999) J Mater Sci 34:2461
20. Tazaki K, Tiba T, Aratani M, Miyachi M (1992) Clay Clay Miner 40:122
21. Stolper E (1982) Contrib Mineral Petr 81:1
22. Lehmann H, Rössler M (1974) Therm Anal 1:619
23. Kamitsos EI, Patsis AP, Karakassides MA, Chryssikos GD (1990) J Non-Cryst Solids 126:52
24. Bertoluzza A, Fagnano C, Morelli MA, Cottardi V, Guglielmi M (1982) J Non-Cryst Solids 48:117
25. Yoshino H, Kamiya K, Nasu H (1990) J Non-Cryst Solids 126:68
26. Kamitsos EI, Patsis AP and Kordas G (1993) Phys Rev B 48:12499; Kamitsos EI (1996) Phys Rev B 53:14659
27. Ingram MD, Davinson JE, Coats AM, Kamitsos EI, Kapoutsis JA (2000) Glastech Ber Glass Sci Technol 73:89
28. Kamitsos EI, Kapoutsis JA, Jain H, Hsieh CH (1994) J Non-Cryst Solids 171:31 and references therein
29. Friedman I, Smith R, Long W (1966) Geol Soc Am Bull 77:323